THE APPLICATION OF THE COMPUTER PROGRAMME TO THE ANALYSIS OF MICROSTRUCTURE OF THE MATRIX OF AUSTEMPERING DUCTILE IRON

Tomasz Giętka, Stanisław Dymski

University of Technology and Life Sciences
al. Prof. S. Kaliskiego 7, 85-789 Bydgoszcz, Poland
tel.: +48 52 3408719, fax: +48 52 3408796
e-mail: tgietka@utp.edu.pl

Abstract

In this work the attempt at quantitative evaluation of the microstructure of ADI cast iron matrix has been made. The automatic analysis of the image of the microstructure of austempered spheroidal cast iron has been used for the evaluation. The treatment variant was a two-phase austenitization. First phase was carried out at a temperature $t_\gamma = 950\ ^0C$ and after cooling to a temperature $t_{\gamma'} = 900\ ^0C$. The isothermal process was carried out at a temperature $t_{pi} = 300$ and $400\ ^0C$ for $8 \div 64$ min. Ordinary cast iron was austempered. After it the microstructure images were recorded and subjected to automatic image analysis with the use of the NIS ELEMENTS 3,0 AR software.

Keywords: Image analysis, Isothermal process, Diffraction, ADI

1. Introduction

In the technology of high strength ADI cast iron grades the microstructure of matrix, consisting of austenite and ferrite [1-3] is significant.

In ADI iron cast production the austempering is used in order to produce high carbon austenite and rich in carbon ferrite in the matrix. Such composition of microstructure is called ausferrite and the isothermal process of over-cooled austenite – ausferritizing.

Research works over ADI cast iron concentrate mostly on ausferritizing process [3, 8, 9-13]. It is a rational approach, because shaping of strength, ductility and toughness as well as impact strength of the cast iron result mostly from the parameters of heat treatment. It is significant on account of the practical cast application in accountable machine parts.

Image analysis is considered to be significant in many fields of science connected to quantitative analysis of microstructure. Application of algorithms of automatic image analysis consists in processing the images of material microstructures in order to calculate statistic characteristics of the size and shape of the grains.

The microstructure which has been analysed in this way may be used to prepare a model of the material structure for simulation calculations with the use of Finite Element Method (FEM). In order to make the calculations reliable, the complex analysis of the input data basing on extraction of characteristic features like edges, inclusions and noise has to be carried out.

The microstructure image analysis is in many cases complex on account of the variety of shapes and sizes of grains, which in effect has an influence on the reliability of the results and the

later calculations [4,6-9]. The majority of accessible algorithms serving to edges detection cannot cope with the problem of occurring noise, treating it as a typical image element.

The aim of this work was to carry out a test of the ADI cast iron components qualitative evaluation with the use of automatic image analysis. The results of the quantitative microscopy have been compared to the X-ray diffraction analysis.

2. Material, programme and research object

The researched cast iron has been smelted in a hot blast cupola furnace. Balling of the cast iron was carried out with the use of magnesium alloy ML5, applying rod method in the container of the cupola. Cast iron has been cast to wet sand moulds. The casts had a shape of ingots YII according to (PN-EN 1563:2000). On the base of static tensile test the cast iron was qualified to the grade EN-GJS-500-7. Cast iron had ferritic- pearlitic (10 %) matrix structure and proper nodular graphite form (share 11,5 %, 112 rel./ mm2 microsection surface).

Chemical composition and properties in the initial state of the ordinary cast iron are presented in the Table 1.

Tab. 1. The chemical composition and mechanical properties in ductile iron

Chemical element, % mas.					
C	Si	Mn	P	S	Mg
3.65	2.59	0.18	0.052	0.014	0.06
Mechanical properties					
R_m, MPa		A_5, %		H, HV10	KCG, J/cm^2
507		12.1		156	106

Before hardening the lower part of ingot YII were treated with two-phase ferritizing annealing. The first phase at the temperature of 1050^0C for 4 hours and the second one after cooling to 680 ^{0}C held for 6 hours. Cooling down of the cut ingots was carried out with the use of a furnace (Fig. 1).
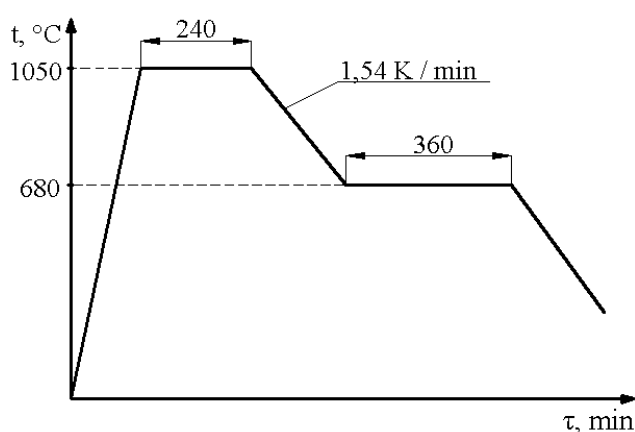

Fig. 1. The schema of dual-stage ferritizing annealing of the ductile cast iron

After that the ingots were cut into three flat bars. The flat bars were marked with the retaining of their previous location in the ingots and the tensile test samples, whose dimensions are depicted in the Figure 2, were made.
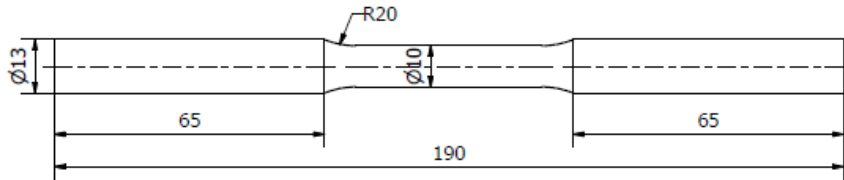
Fig. 2. Dimensions of the tensile test

Tensile test samples have been austempered according to the schemes shown by the Figure 3. For every treatment condition a set consisting of 3 samples, originating from 1 ingot YII, has been prepared.

From the gripping part of the samples after heat treatment the 11-millimetre-long specimens were taken, on which metallographic microsections were made. They served for the assessment of their microstructure under an optic microscope. The record of the microstructure images has been made with the use of scanning electron microscope (SEM) type JSM-50A made by company JEOL with the acceleration voltage 20 kV and absorptive current of the sample ca. $0{,}2 \cdot 10^{-10}$ A. The images have been registered on the enlargement scale $1000 \div 3000$x.
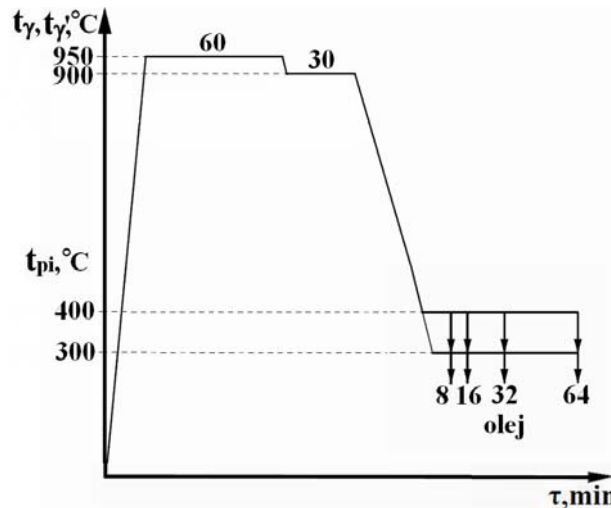

Fig. 3. Scheme depicting austempering of the ductile cast iron

Automatic image analysis has been made with the use of NIS ELEMENTS 3,0 AR software (Fig. 4). Its task was to calculate specially marked pixels of the image which was calibrated according to the enlargement. Halftone screen image received from the scanning microscope has been converted to the binary image, which explicitly determined the evaluated microstructure components. With the use of computer software the share of austenite and sizes of the ferrite needles have been determined.
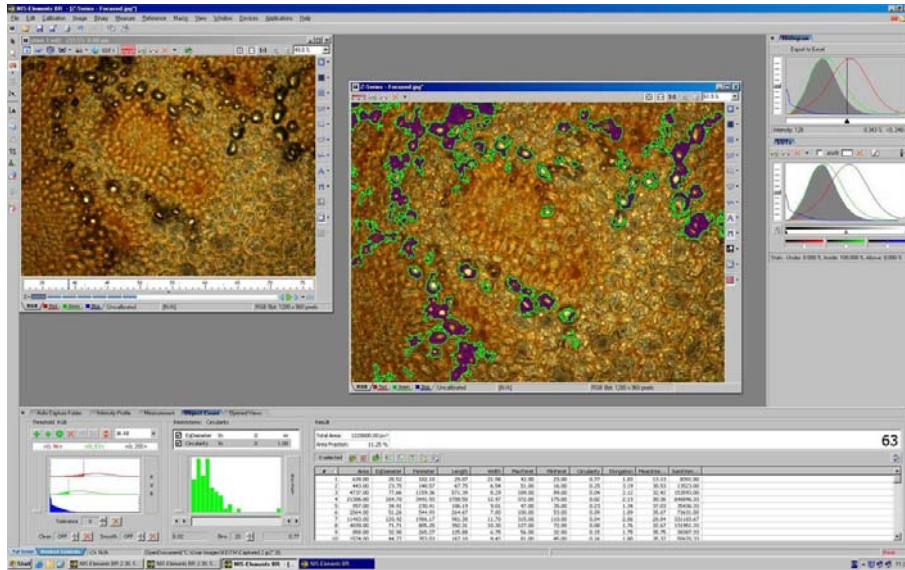
Fig 4. The window of the programme NIS ELEMENTS 3,0 AR

On the metallographic specimens also the x-ray diffraction analysis has been carried out. The research has been made on the diffractometer, using CoKa radiation and iron filtering. The following parameters of diffractometer's work have been assumed:

- lamp voltage 36 kV;
- lamp current 6 mA;
- the arrangement of collimating slits I – 2, II – 2, III – 2 mm, the Soller slits on the primary beam and on the diffracted beam;
- scintillation counter detector operated at 700 V.

Diffraction patterns have been recorded within the angular range 2Θ $49,5 \div 53,5^0$. Within this angular range, using step $0,01^0$, diffraction lines (110) phases α and (111) and phases γ have been recorded. Intensity of each interference line has been determined three times by planimetring of the field under the curve to the background level. Share of austenite (V_γ) from the formula 1 [17]:

$$V_\gamma = \frac{1}{1 + I_\alpha \cdot I_\gamma^{-1} \cdot R} \cdot 100 \text{ \%}$$

(1)

where:

V_γ - share of austenite in the volume fraction,

I_α - relative intensity of diffraction line (110) phase a, planimetred on the X-ray photograph,

I_γ - relative intensity of diffraction line (111) phase γ, planimetred on the X-ray photograph,

R - value of the constant accepted to these measurements 0,85. mm

Averaging size of ferrite needles has been determined from the formula 2 [18]:

$$d = \frac{0,9 \cdot \lambda}{B \cdot \cos \Theta}$$

(2)

where:

d - average diameter of the crystal particle,

λ - wavelength in nm,

B - diffraction line broadening, measured in the middle of its maximal intensity in rad,

Θ - the angle of the interference line determined from the diffraction pattern in ^{0}.

## 3. The results of the research and their analysis

The quantitative evaluation of the components of the austempered cast matrix microstructure has been carried out on 5 random chosen images, registered for each specimen which has been enlarged 2000x. The demonstration microstructures of the cast iron have been depicted in the Figures 5 ÷ 8.
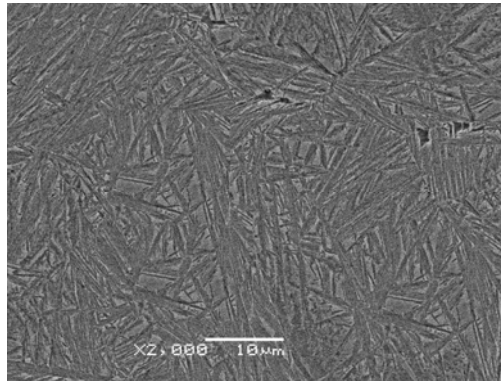
Fig. 5. The microstructure of the cast iron austempered at a temperature $t_{pi} = 300\ ^0C$, $\tau_{pi} = 8$ min. Etched in nital, micr. surf. 2000x
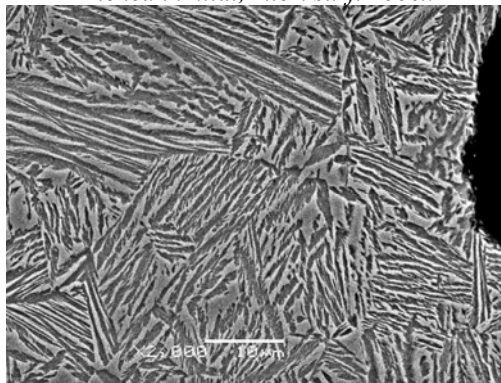
Fig. 6. The microstructure of the cast iron austempered at a temperature $t_{pi} = 400\ ^0C$, $\tau_{pi} = 8$ min. Etched in nital, micr. surf. 2000x
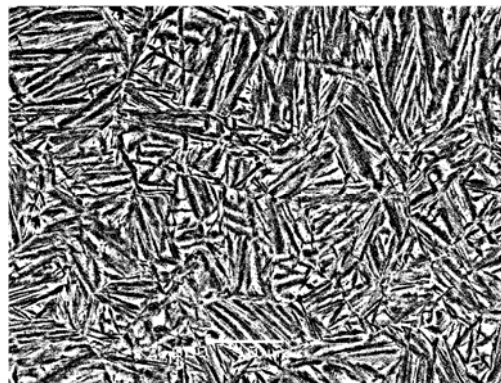
Fig. 7. Binary image of the cast iron microstructure austempered at a temperature $t_{pi} = 300\ ^0C$, $\tau_{pi} = 64$ min. Etched in nital, micr. surf. 2000x

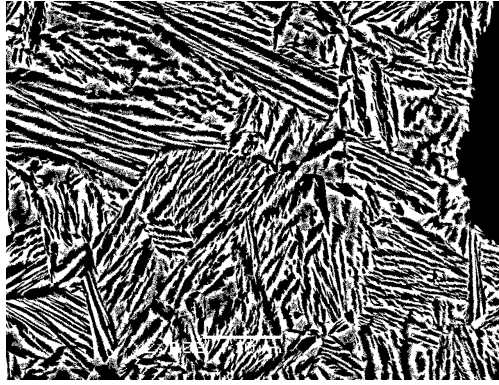*Fig. 8. Binary image of the cast iron microstructure austempered at a temperature t_{pi} = 400 ^{0}C, τ_{pi} = 8 min. Etched in nital, micr. surf. 2000x*

After austempering at temperature t_{pi} = 300 ^{0}C the matrix consisted of the lower ausferrite (Fig. 5, 7). While at a temperature t_{pi} = 400 ^{0}C upper ausferrite (Fig. 6, 8). The morphology of the components of ADI cast iron microstructure has been changing in the holding time function. For comparison the microstructure registered on (SEM) for the specimen austempered at a temperature t_{pi} = 300 ^{0}C for 8 minutes (Fig.5) as well as the binary image of the specimen austempered at the same temperature for 64 minutes (Fig. 7). With the elongation of the conversion time the ferrite needles have undergone the length change and the austenite plates have been evenly distributed. The conversion time affects the microstructure arrangement.
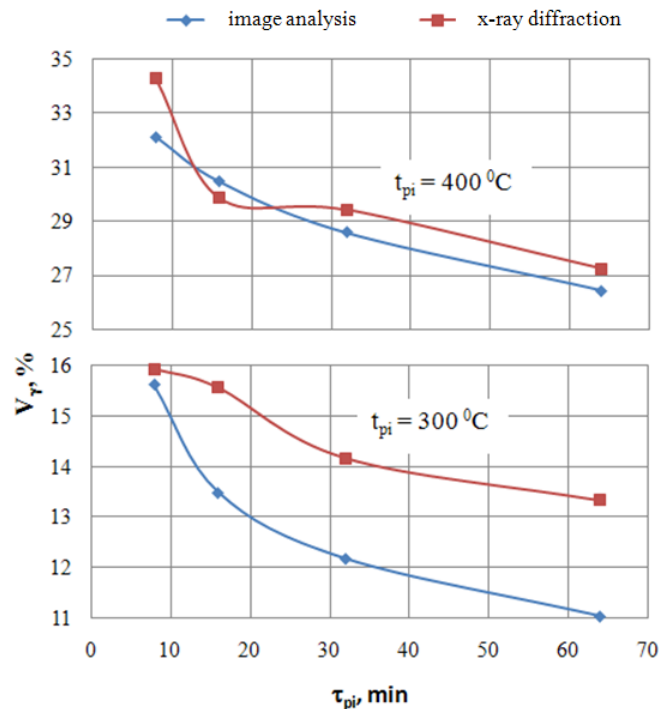

Fig. 9. Impact of the temperature and austempering time on the austenite share (V_γ)) in the ADI cast iron matrix

On the base of image analysis the share of austenite in the microstructure has been determined. The microstructure of the ADI cast iron austempered at a temperature t_{pi} = 400 ^{0}C contained austenite in the range 32,1 ÷ 26,4 % while at a temperature t_{pi} = 300 ^{0}C - 15,6 ÷ 11,0 %. The share of phase γ determined by diffraction was bigger for both temperatures (apart from τ = 16 min for t_{pi} = 400 ^{0}C). The character of the chart lines was the same for both research methods. The growth of conversion time caused a decrease of the austenite share. The differences of the received results

depicting the austenite share in the cast iron matrix were bigger for the lower temperature of austempering. It results from finer microstructure of the matrix.
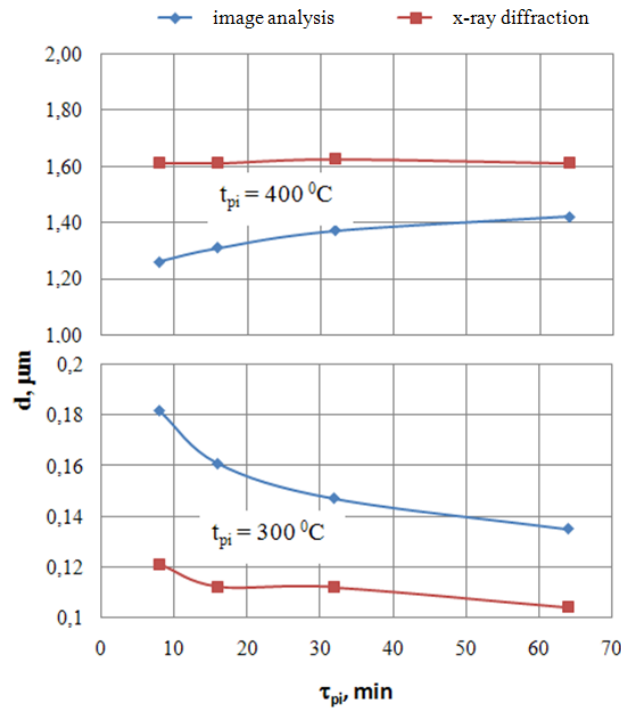

Fig. 10. Impact of the temperature and isothermal process time on the average diameter of the ferrite needles (d) in ADI cast iron matrix.

The diameter of the ferrite needles (Fig. 10) measured by image analysis is almost ten times, and with the use of diffraction thirteen times smaller at 300 ^{0}C than at 400 ^{0}C. The little transverse size of the ferrite needles in lower ausferrite has contributed to registering low contrasted images. The result of it has been depicted in the figure 10 between the diameters at – values determined from the image analysis and the diameters at – values received from the rtg diffraction for t_{pi} = 300 ^{0}C. Bigger diameters at – sizes received from the image analysis result from binary images which have been enlarged by noise and shadows. The change of the transverse sizes of the ferrite needles is connected to the conversion $\gamma \rightarrow \alpha$ mechanism.

The length of the ferrite needles in ADI cast iron under the influence of time decreased (Fig. 11). This relation is stronger in cast iron which has been hardened from the temperature t_{pi} = 300 ^{0}C than at – 400 ^{0}C.
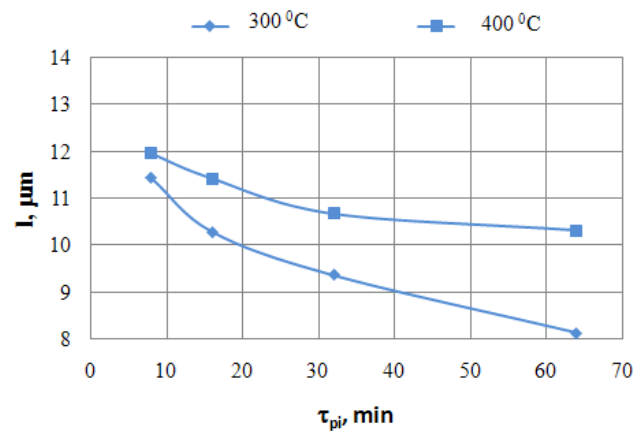

Fig. 11. Impact of the temperature and isothermal process time on the length of the ferrite needles determined with the use image analysis software

ε

4. Conclusion

On the base of the research carried out and its results the following statements can be made:

1. The image analysis software NIS ELEMENTS 3,0 AR can be used to the quantitative evaluation of the components of ADI cast iron matrix microstructure.
2. From the comparison of methods to the evaluation of the percentage share of austenite in ADI it results that the computer image analysis can be used in the upper ausferrite examination. However, in the range of the lower ausferrite the measurement discrepancy between the methods rises to over 2%.
3. The evaluation of the sizes (diameters and length) of the ferrite needles in ausferrite has been treated as a pre-operation to the next research, although during the analysis of the received results the meaningful impact of the temperature and austempering time on these sizes has been noticed.

References

[1] Pietrowski, S., *Żeliwo sferoidalne o strukturze ferrytu bainitycznego z austenitem lub bainitycznej*, Archiwum Nauki o Materiałach, t.18, pp. 253-273, 4/1997.

[2] Guzik, S. E., *Żeliwo ausferrytyczne jako nowoczesne tworzywo konstrukcyjne*, Inżynieria Materiałowa, pp. 677-680, 6/2003.

[3] Dymski, S., *Kształtowanie struktury i właściwości mechanicznych żeliwa sferoidalnego podczas izotermicznej przemiany bainitycznej*, Rozprawy nr 95. ATR Bydgoszcz, 1999.

[4] Wojnar, L., Kurzydłowski, K., Szala, J., *The Practician of the Analysis of the Painting*, Publishing house Polish Company Stereology, Cracow, 2002.

[5] Kovacs, B. V., *On the Terminology and Structure of ADI*, AFS Transactions, pp. 417-420, 102/1994.

[6] Miernik, K., Bogucki, R., Gądek, A., Dziadur, W., *The Influence of Conditions of the Thermal Processing on Content of the residual austenite in Ductile Cast Iron of Ishothermal Transformation (ADI)*, Conference Materials XXX the School Engineering Material, Kraków-Ustroń Jaszowiec, 2002.

[7] Szala, J., *The computer analysis of the painting in metallography quantitative*, The Programmer in the Technology Metals, vol. 3, pp. 41-57, 1/2003.

[8] Kowalski, A., Kuder, M., *Use of Computer Programme to the Analysis of Painting LUCIA to the Quantitative Opinion of the Structure of Cast Iron ADI*, Innovations in Founding, Part I, Cracow, pp. 281-290, 2007.

[9] Rauch, Ł., Kusiak, J., *Automatic Analysis of Microstructure Photographs*, Scientific Works, Varsovian Engineering College z. 216, pp. 165–170, 2007.

[10] Kilicli, V., Erdogan, M., *The Strain-Hardening Behavior of Partially Austenitized and the Austempered Ductile Irons with Dual Matrix Structures*, Journal of Materials Engineering and Performance, vol. 17, pp. 240-249, 2/2008.

[11] Delia, M., Alaalam, M., Grech, M., *Effect of Austenitizing Conditions on the Impact Properties of an Alloyed Austempered Ductile Iron of Initally Ferritic Matrix Structure*, vol 7, pp. 265 – 272, 2/1998.

[12] Grech, M., Young, J. M., *Effect of Austenitising Temperature on Tensile Properties of Cu-Ni Austempered Ductie Iron*, Materials Science and Technology, pp. 415-421 6/1990.

[13] Mallia, J., Grech, M., *Efect of Silicon Content on Impact Properties of Austempered Ductile Iron*, Materials Science and Technology, pp. 408-414, 13/1997.

[14] Ogi, K., Sawamoto, A., Jin, Y. C., Loper Jr. C. R., A Study of Some Aspects of the Austenitization Process of Spheroidal Graphite Cast Iron, AFS Transactions vol. 96 (1988).

[15] Aranzabal, J., Gutierrez, I., Rodriguez-Ibabe J. M., Urcola J. J., *Influence of the Amount and Morphology of Retained Austenite on the Mechanical Properties of an Austempered Ductile Iron*, Metallurgical and Materials Transactions, pp. 1143-1156, 28A/1997.

[16] Eric, O., at al., *The Austempering Study of Alloyed Ductile Iron*, Materials   Design, pp. 617-622, 27/2006

[17] Senczyk, D., *The Laboratory from X-Ray Structure Analysis*, Pub. School Engineering, Poznań, 1974.

[18] Cullity, B. D., *Elements of X-Ray Diffraction*, State Scientific Publishing house, Warsaw, 1964